Magnesium Technology 2013
Edited by: Norbert Hort, Suveen N. Mathaudhu, Neale R. Neelameggham, and Martyn Alderman
TMS (The Minerals, Metals & Materials Society), 2013

PHASE STABILITY INVESTIGATION OF THE MG-ZN-SM SYSTEM

Xiangyu Xia[1], Amirreza Sanaty Zadeh[1], Chuan Zhang[2], Xiaoqin Zeng[3], Donald Stone[1], Alan.A. Luo[4]
[1] Materials Science Program; University of Wisconsin, Madison; 1509, University Ave; Madison, WI, 53706, USA
[2] Computherm LLC, 437 S. Yellowstone Dr, Suite217, Madison, WI, 53719, USA
[3] Department of Materials Science and Engineering; Shanghai Jiaotong University; 800, Dongchuan Road, Shanghai, 200240, China
[4] Chemical and Materials Systems Laboratory; General Motors Research and Development Center; 30500 Mound Road, Warren, MI, 48090, USA

Keywords: Mg-Zn-Sm system; intermetallics; isothermal section

Abstract

Phase equilibrium of the Mg-Zn-Sm ternary system at the Mg-rich region at 400°C was investigated. One ternary phase Z was confirmed, with a composition formula of $Mg_3Zn_{10}Sm$ and crystal structure of $P6_3/mmc$. Zn was found to have large solubility in both Mg_3Sm (~35.6 wt.%) and $Mg_{41}Sm_5$ (~4 wt.%) phases. An isothermal section of 400°C in the Mg-rich corner was constructed, which provides important understanding of phase relationships in the Mg-Zn-Sm system.

Introduction

Magnesium alloys have been increasingly used in the automotive and aerospace industries for light weighting and energy saving, because of their low density, high specific stiffness, excellent castability, and other favorable attributes [1-4]. However, the relatively poor mechanical properties like strength and creep resistance have limited their applications. The addition of Zn has been reported to significantly enhance strength and creep resistance in Mg alloys by both solid solution strengthening and age hardening. However, Zn also brings brittleness and coarse grains [5], so a third strengthening element is always considered in Mg-Zn alloys. Mg-Zn-RE (rare earth) alloys have attracted much interest recently. RE's solid solution strengthening in α(Mg) and precipitation strengthening from the intermetallics could provide strong influence on Mg alloy mechanical properties[6,7].

Samarium (Sm), as one of the cheapest RE elements, attracts significant interest. Although there have been some reported studies on the mechanical properties of Mg-Zn-Sm alloys [8,9,10], the strengthening mechanisms, intermetallics and phase diagrams are yet to be fully understood. Drits, et al [11] studied the phase relationships in this system, as well as liquidus projection and a partial isothermal section at Mg corner, as shown in Fig.1. Three ternary phases X ($(Mg_{1.39}Zn_{0.62})_3Sm_2$), Y ($Mg_{9.54}Zn_{5.21}Sm$), Z ($Mg_3Zn_6Sm$) were also identified. However, their study was not sufficient for further applications for the following reasons: 1) The homogeneity ranges of the three ternary phases were not clearly specified; 2) Despite the clear crystal structure information for X (FCC, a=6.994Å) and Z (HCP, a=14.62 Å, c=8.78 Å) phase, such information for Y phase was not available; 3) These three phases differ significantly in composition and crystal structure from those investigated in [12-14], which are named as μ_3 ($Mg_{13}Zn_{30}Sm_3$), μ_5 ($Mg_{15}Zn_{40.5}Sm_{6.5}$) and μ_7 ($Mg_{58.1}Zn_{155.3}Sm_{26.6}$), all with hexagonal crystal structure. Thus, a detailed investigation into ternary phases and phase relationships in this system is necessary.

For this purpose, three typical Mg-Zn-Sm alloys (their compositions are listed in Table. 1) were identified for experimental investigation based on the work of Drits et al [11]. As shown in Fig.1, the alloys selected in this study are located in the three-phase region, which will provide us with more phase-equilibrium information and less experimental work. In this study, phase equilibria of these three alloys at 400°C were investigated.

Experimental

The Mg-Zn-Sm alloy samples were prepared using commercially pure Mg, Zn (>99.9wt%) and Mg-20wt.%Sm master alloy ingots. Melting process was under protection of SF_6/CO_2 and the samples were cut into pieces of around 100g. The chemical composition of each alloy was then analyzed using Inductively Coupled Plasma Mass Spectrometry (ICP-MS) and listed in Table.1. Afterwards, samples were wrapped with tantalum foils respectively, sealed in a quartz tube and back-filled with high-purity argon atmosphere (>99.999%), and then annealed at 400°C for one month. Phase identification and lattice parameter measurements were performed by X-ray diffraction (XRD) using General Area Diffraction Detector System (GADDS), with Cu Kα radiation (40kV, 50 mA), as well as Transmission Electron Microscopes (TEM, Tecnai T12). SEM (EVO-50) was employed to study the microstructures. The compositions of each element within the phases in equilibrium were determined using Electron Probe Microscope Analysis (EPMA) (CAMECA SX100).

Table.1. Chemical composition of selected Mg-Zn-Sm alloys and EPMA measured compositions of each phase in equilibrium from this study (the chemical composition is measured by ICP)

Alloy #	Overall Compositions (wt.%)	Phases	Mg (wt.%)	Zn (wt.%)	Sm (wt.%)
1	Mg-23.35Zn-5.73Sm	α(Mg)	90.2	9.7	0.1
		Z	12.43	70.16	17.76
2	Mg-1.17Zn-	α(Mg)	97.19	0.36	1.70

	13.01Sm	$Mg_{41}Sm_5$	54.71	3.88	40.64
3	Mg-8.16Zn-13.38Sm	α(Mg)	97.17	0.8	1.10
		Mg_3Sm	12.36	35.59	50.13

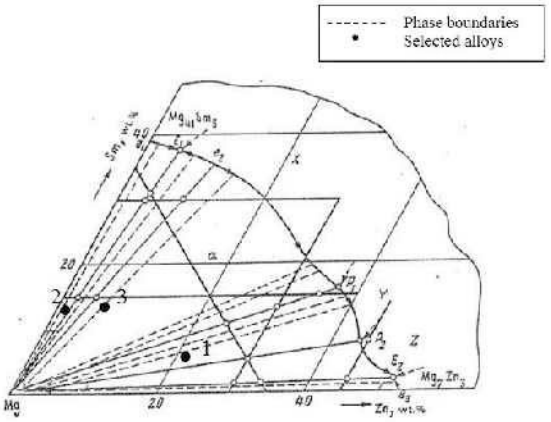

Fig.1. Projection of crystallization surfaces, and phase regions at 300°C of Magnesium corner of system Mg-Sm-Zn [11]

Results and Discussion

A typical microstructure of alloy #1 Mg-23.35Zn-5.73Sm is shown in Fig.2.a. Two phases are in equilibrium: white dendritic phase and dark matrix. The XRD results shown in Fig.3 indicate that the α (Mg) and Z phase coexist. The compositions of either phase determined from EPMA are listed in Table.1. Based on the above phase identification results, the dark matrix is α(Mg), in which Zn has a solubility of around 9.7 wt%; the light Z phase has a composition of Mg-72Zn-16.5Sm and a formula of $Mg_3Zn_{10}Sm$. The XRD pattern corresponds well with the hexagonal phase μ_3, with the lattice constants a=14.6Å and c=8.71Å.

It should be noted that though μ_3, μ_5, μ_7 [12-14] are three individual phases, they are similar in many perspectives: same crystal structures ($P6_3/mmc$), same "c" lattice constant (8.8Å), similar composition (Mg: Zn: Sm≈3:10:1) and the only difference is the "a" lattice parameter (14.6Å/23.5Å/33.6Å). For our purpose of constructing Mg-Zn-Sm phase diagram around Mg-rich corner and further assisting alloy optimization, it would be difficult and unnecessary to distinguish these three phases; thus we take the average composition for Z phase, while the crystal structure resembles that of μ_3.

The BSE image of alloy #2 Mg-1.17Zn-13.01Sm is presented in Fig.2.b. The dark phase is identified to be α(Mg), with 1.7% Sm and negligible Zn. The light phase corresponds well to $Mg_{41}Sm_5$, with a solubility of Zn of around 4%, as listed in Table.2. The existence of these two phases is supported by the XRD spectrum as seen in Fig.3. Compared with $Mg_{41}Nd_5$ [16], $Mg_{41}Sm_5$ has the same crystal structure (I4/m), similar lattice constants ($Mg_{41}Sm_5$: a=14.8Å, c=10.36Å; $Mg_{41}Nd_5$: a=14.7Å, c=10.40Å) and similar Zn solubility (~2-3%), thus it is reasonable to infer that Zn's substitution mechanism would be the same in both phases, which means Zn substitute Mg atoms in $Mg_{41}Sm_5$.

The BSE image in Fig.2.c shows the two phase equilibrium in alloy #3 Mg-8.16Zn-13.38Sm. The dark matrix is α(Mg) and the eutectic white is identified to be Mg-35.6Zn-50Sm, i.e. the X phase [11]. The formula is calculated as $Mg_{34.1}Zn_{36.6}Sm_{22}$. The eutectic structure indicates an eutectic reaction L = X + Mg, as described in Drits'[11] and the eutectic dark phase is eutectic Mg. The presence of the two phases is confirmed by the XRD pattern in Fig.3.

Fig. 4 shows the bright field image of the X phase and the selected area diffraction patterns from two different zone axes. The crystal structure of the X-phase is confirmed to be FCC, as it was found from the XRD patterns.

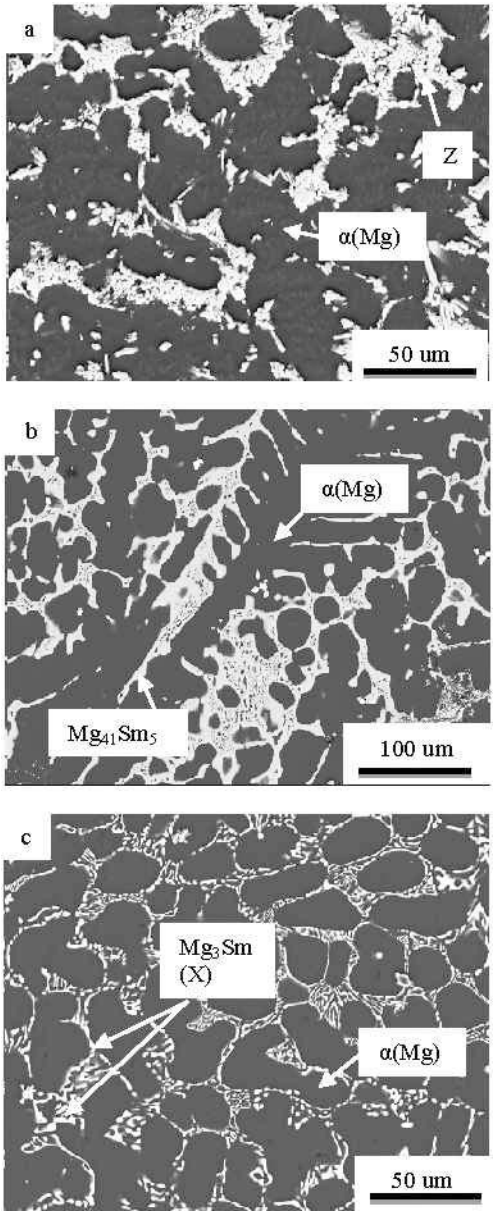

Fig.2. BSE images of Annealed Alloys ((a):#1;(b):#2; (c):#3)

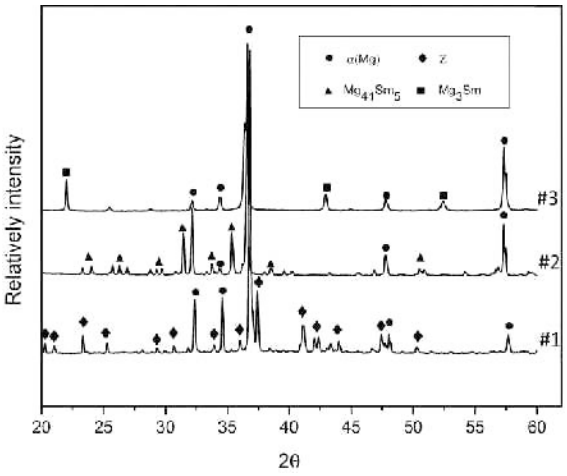

Fig.3. XRD Patterns of Annealed Alloys

The lattice parameter, calculated from the diffraction patterns for X-phase is between 6.64-6.94 Å. These values are consistent with the calculated values from the XRD patterns, i.e. 6.97Å. The lower value for lattice parameter, compared to that of Mg_3Sm (a=7.731Å) [17], is probably caused by magnesium atoms, with larger atomic radius, being randomly replaced with smaller zinc atoms in the structure. Therefore, while the X-phase was proposed to be $((Mg_{1.39}Zn_{0.62})_3Sm_2)$ in an early study [11], the XRD and TEM results in this paper, along with the fact that the composition of Mg and Zn together is 3 times as that of the Sm, suggest that this phase is instead the Mg_3Sm binary phase with a large solubility of zinc atoms in the structure.

Based on the above results, a schematic isothermal section of Mg-Zn-Sm system in Mg-rich corner at 400°C is determined, as shown in Fig.5.

In alloy#1, only two phases exist, indicating that #1 is either on the α(Mg)-Z tie-line, or the amount of Mg_7Zn_3 or Mg_3Sm is too small to be detected. In either situation, the tie-line between α(Mg) and Z phase would be close to #1's composition. The limited homogeneity is represented by the dashed circles.

In #2, $Mg_{41}Sm_5$ contains around 4% of Zn. Thus its homogeneity range expands towards Zn corner and #2 lies within the two phase region. #3 lies in the α(Mg)-Mg_3Sm region. The α(Mg)-Mg_3Sm-$Mg_{41}Sm_5$ ternary region can be inferred from phase rule, shown as dashed lines in Fig.5.

The ternary region α(Mg) + Mg_3Sm + Z was not observed from present experimental results. However its boundary can be estimated from compositions of Z and Mg_3Sm, and labeled as dashed lines in Fig.5. Further study with more selected alloys under different annealing temperatures is undergoing to clarify phase equilibria at the Mg-rich corner of the Mg-Zn-Sm ternary system. .

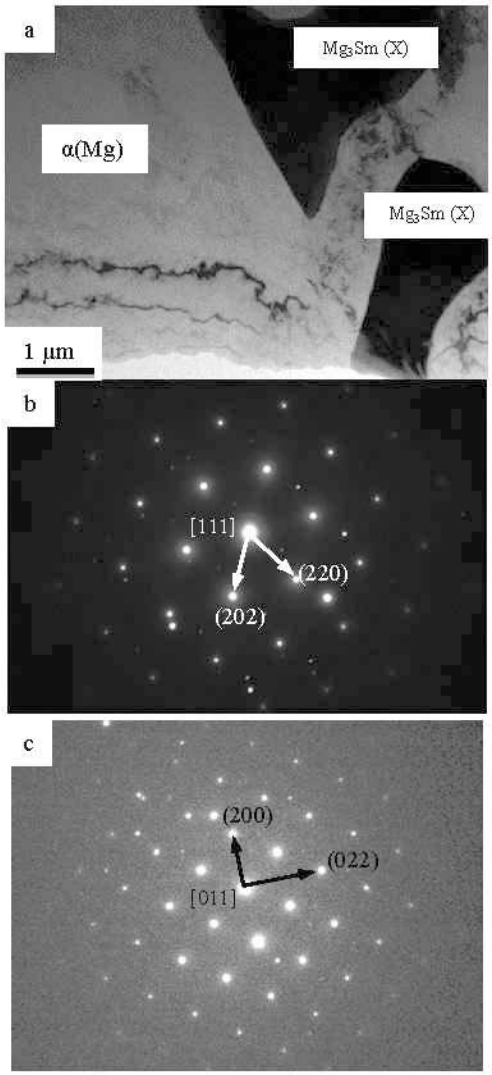

Fig.4. (a). TEM BF image of alloy #3 Mg-8.16Zn-13.38Sm; (b). TEM SAD pattern of Mg_3Sm (X-phase) with zone axis B = [111]; (c). TEM SAD pattern of Mg3Sm (X-phase) with zone axis B = [011].

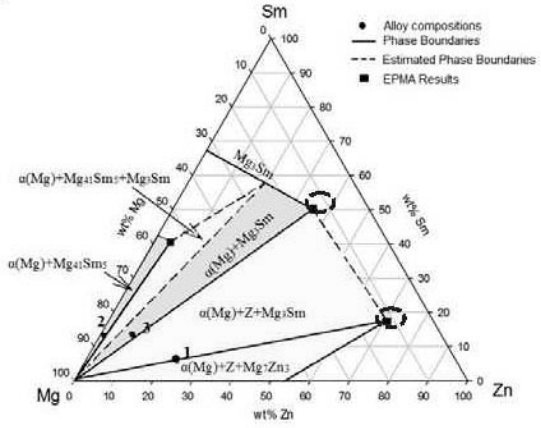

Fig.5. Isothermal section of Mg-Zn-Sm system in Mg corner at 400°C

Conclusions

1. The ternary phase Z was confirmed, with a modified formula of $Mg_3Zn_{10}Sm$ and hexagonal structure.

2. The solubility of Zn in binary phase $Mg_{41}Sm_5$ in 400°C is estimated as 4%. The crystal structure remains the same.

3. The X-phase identified by Drits [11] is experimentally confirmed to be the binary Mg_3Sm phase with the solubility of Zn around 35.6% along the Mg-Zn binary direction.

4. Three binary phase equilibriums α(Mg)+Z, α(Mg)+$Mg_{41}Sm_5$, α(Mg)+Mg_3Sm were identified and partial isothermal section of Mg-Zn-Sm at 400°C was constructed.

Acknowledgements

The authors wish to thank Anil Sachdev, Rick Waldo and Misle Tessema from General Motors Global R&D for helpful discussion and technical support, Shanghai Jiaotong University for sample preparation and the financial support from the National Science Foundation (No. 1005762).

References

1. M. Bamberger, G. Dehm, "Trends in the Development of New Mg Alloys", Annu. Rev. Mater. Res. 2008. 38, p. 505-33.

2. A.A.Luo, "Recent magnesium alloy development for elevated temperature applications", International materials reviews, 2004, P. 13-30.

3. M. O. Pekguleryuz, A.A. Kaya. In: K.U. Kainer, editor. Magnesium alloys and their Applications. Germany, Wiley-VCH Verlag GmbH, (2003), p. 74.

4. A. A. Luo, R. K. Mishra, etc, "Magnesium Alloy Development for Automotive Applications", Materials Science Forum, 2012, 706-709, p. 69-82.

5. C.J. Boehlert, "The tensile and creep behavior of Mg-Zn Alloys with and without Y and Zr as ternary elements", J Mater Sci, 2007, P. 3675-3684.

6. L. L. Rokhlin, Magnesium Alloys Containing Rare Earth Metals: Structure and Properties. CRC Press, 2003

7. I. P. Moreno, T. K. Nandy, etc, "Microstructure and Creep Behavior of a Die Cast Mgnesium-Rare Earth alloy", Magnesium Technology 2002, p. 111-116.

8. Rokhlin L. L, "PHASE DIAGRAM AND MECHANICAL PROPERTIES OF Mg-Sm ALLOYS", Russian Metallurgy, 1979, 4, p. 165-167.

9. L. L. Rokhlin, S.V. Dobatkin, etc, "Effect of Severe Plastic Deformation on the Structure and Properties of the Age-Hardenable Mg-Sm Alloys", Materials Science Forum, 2006, 503-504, p. 961-966.

10. N. P. Abrukina, "MICROHARDNESS OF PHASES IN THE SYSTEMS Mg-Sm-Y and Mg-Sm-Zn", Russian Metallurgy, 1987, 2, p. 210-212.

11. M. E. Drits, L. L. Rokhlin, etc, "PHASE EQUILIBRIUM IN THE Mg-Sm-Zn SYSTEM", Russian Metallurgy, 1985, 6, p. 194-200.

12. Kazumasa Sugiyama, etc, "Crystal structure of μ_7-MgZnSm", Journal of Alloys and Compounds, 1999, 285, p. 172-178.

13. E. Abe, H. Takakura, etc, "Hexagonal superstructures in the Zn-Mg-rare-earth alloys", Journal of Alloys and Compounds, 1999, 283, p. 169-172.

14. K. Sugiyama, K. Yasuda, etc, "The structure of hexagonal phases in Mg-Zn-RE (RE=Sm and Gd) alloys", Z. Kristallogy, 1998, 213, p. 537-543.

15. Pandat 8.0 – Phase Diagram Calculation Software for Multi-component Systems, Computherm LLC, 437 S. Yellowstone Dr, Suite217, Madison, WI, 53719, USA, 2008.

16. Guo. C, etc, Mg-Nd Phase Diagram, ASM Alloy Phase Diagrams Center, P. Villars, editor-in-chief; H. Okamoto and K. Cenzual, section editors; http://www1.asminternational.org/AsmEnterprise/APD, ASM International, Materials Park, OH, 2006

17. Okamoto H, etc, Mg-Sm Phase Diagram, ASM Alloy Phase Diagrams Center, P. Villars, editor-in-chief; H. Okamoto and K. Cenzual, section editors; http://www1.asminternational.org/AsmEnterprise/APD, ASM International, Materials Park, OH, 2006